Asymmetries between Wavenumber Spectra of Along- and Across-Track Velocity from Tandem Mission Altimetry

CIMARRON WORTHAM

Applied Physics Laboratory, University of Washington, Seattle, Washington

JÖRN CALLIES

Massachusetts Institute of Technology/WHOI Joint Program in Oceanography, Cambridge, Massachusetts

MARTIN G. SCHARFFENBERG

Institut für Meereskunde, Universität Hamburg, Hamburg, Germany

ABSTRACT

Satellite altimetry has proven to be one of the most useful oceanographic datasets, providing a continuous, near-global record of surface geostrophic currents, among other uses. One limitation of observations from a single satellite is the difficulty of estimating the full geostrophic velocity field. The 3-yr *Jason-1*–Ocean Topography Experiment (TOPEX)/Poseidon tandem mission, with two satellites flying parallel tracks, promised to overcome this limitation. However, the wide track separation severely limits the tandem mission's resolution and reduces the observed velocity variance. In this paper, the effective filter imposed by the track separation is discussed and two important consequences for any application of the tandem mission velocities are explained. First, while across-track velocity is simply low-pass filtered, along-track velocity is attenuated also at wavelengths much longer than the track separation. Second, velocity wavenumber spectral slopes are artificially steepened by a factor of k^{-2} at wavelengths smaller than the track separation. Knowledge of the effective filter has several applications, including reconstruction of the full velocity spectrum from the heavily filtered observations. Here, the hypothesis that the tandem mission flow field is horizontally nondivergent and isotropic is tested. The effective filter is also used to predict the fraction of the eddy kinetic energy (EKE) that is captured for a given track separation. The EKE captured falls off rapidly for track separations greater than about 20 km.

1. Introduction

Estimation of the geostrophic surface flow field is one of the major justifications for satellite altimetric missions. The across-track velocity component can be estimated at about 50-km resolution from a single altimeter mission. However, estimates of the full velocity field require computing the gradient in two directions, either by mapping the data, using points where two satellite tracks cross (crossover point analysis), or using two simultaneous altimetric measurements (parallel-track method).

The parallel-track method was described by Stammer and Dieterich (1999) and the expected uncertainty for all three methods were analyzed (Leeuwenburgh and Stammer 2002; Schlax and Chelton 2003). Recently, results from the *Jason-1*–Ocean Topography Experiment (TOPEX)/Poseidon (JTP) tandem mission were analyzed with the parallel-track method to estimate the surface geostrophic flow field (Stammer and Theiss 2004; Scharffenberg and Stammer 2010, 2011).

Both along- and across-track velocities are underestimated by the JTP tandem mission due to the wide track separation (Leeuwenburgh and Stammer 2002). However, for the along-track component, velocity spectra are underestimated even at wavelengths much larger than the track separation. In this paper, we compare spectra of along- and across-track velocities in the western

Corresponding author address: Jörn Callies, Massachusetts Institute of Technology, 77 Massachusetts Ave., Cambridge, MA 02139.
E-mail: joernc@mit.edu

subtropical Atlantic from three sources: monomission and tandem mission altimetry as well as shipboard acoustic Doppler current profiler (ADCP) velocity from the Oleander project (Flagg et al. 1998; Wang et al. 2010). While the spectra of across-track velocity from monomission altimetry and ADCP are consistent with each other, the tandem mission spectrum of along-track velocity is weaker than the ADCP estimate by a factor of 2.5, even at the longest resolved wavelengths.

An explanation of the missing variance in the tandem mission estimates is presented based on the effective filtering of the two-dimensional wavenumber spectrum of sea surface height (SSH) due to the track spacing. The counterintuitive impact of track spacing on the velocity estimates has important consequences for the interpretation of existing data and for the design of future altimetric missions.

2. Observed wavenumber spectra

As an illustration of the too weak velocity spectrum calculated from the JTP tandem mission altimetry, along-track wavenumber spectra from several sources are compared. Data considered here are from the Gulf Stream region spanning 33°–40°N, 288°–295°E. This region is chosen because nearly coincident satellite and in situ observations allow the most direct comparison of velocity estimates, and because the strong SSH variability in the region increases the signal-to-noise ratio for the altimetric results. All spectra are for velocity in the along- or across-track directions relative to the ship or satellite track, rather than zonal and meridional.

a. Shipboard ADCP

We use 11 yr (1994–2004) of ADCP data collected by the Oleander project. Data are from a narrowband 150-kHz ADCP mounted in the hull of the Motor Vessel (M/V) *Oleander* and collected during the container ship's weekly round-trip transit between Port Elizabeth, New Jersey, and Hamilton, Bermuda (Flagg et al. 1998). Data are 10-min averages, resulting in an average horizontal resolution of 4.8 km. In the vertical, data are averaged over the depth range 25–35 m.

In this analysis, we use only transits with data spanning more than 1000 km and with at least 90% data coverage. These criteria result in 481 usable transits. For each transit, velocity is first rotated into along- and across-track coordinates and then interpolated to a regular 5-km grid along the ship track using cubic-spline interpolation. Finally, the time-mean velocity is subtracted at each point along the interpolated track.

The discrete Fourier transform of velocity is computed for each transit after removing the spatial mean
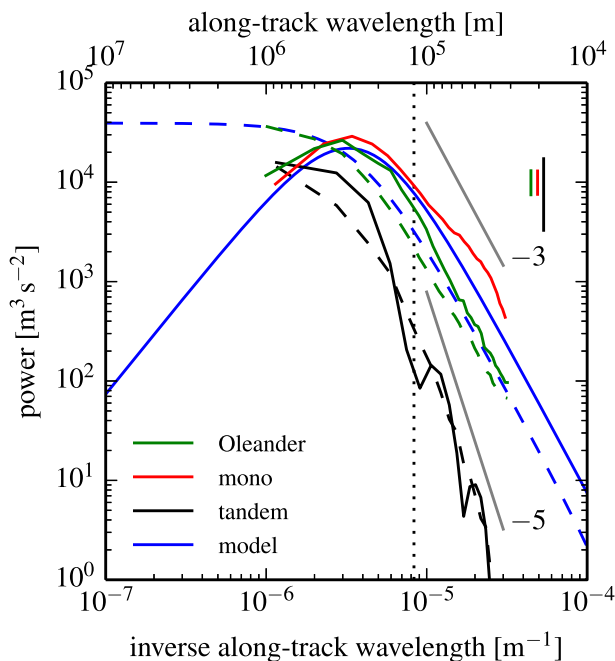

FIG. 1. Along-track wavenumber spectra of across- (solid lines) and along-track (dashed lines) velocity from *Oleander* ADCP measurements (green), monomission altimetry (red), and JTP tandem mission altimetry (black). The analytical spectrum model (blue) is discussed in section 3. The vertical dotted line shows the JTP tandem mission track separation. Power laws with slope k^{-3} and k^{-5} are shown for reference (gray lines). Vertical bars show 95% confidence intervals.

and tapering with a Hamming window. Finally, the spectrum for each velocity component is calculated by averaging over all transits (Fig. 1).

There are important differences between the spectra of along- and across-track velocity. The spectrum of along-track velocity is red over the full wavelength range, while the spectrum of across-track velocity has a peak near 300 km. This difference is expected based on the kinematics of homogeneous, isotropic turbulence (Batchelor 1953; Leith 1971; Callies and Ferrari 2013). At wavelengths shorter than 100 km, the spectrum of both velocity components approaches a k^{-3} power law, where k is the along-track wavenumber.

b. Monomission altimetry

The 15 yr (1993–2007) of SSH data from TOPEX/Poseidon (TP) and its replacement *Jason-1* (*J1*) are used to estimate the wavenumber spectrum of the across-track geostrophic velocity in the vicinity of the *Oleander* ship track. The closest satellite tracks (passes 50 and 126) over the latitude range 33°–40°N are used. These passes are nearly parallel to the *Oleander* track, but rotated by 17° relative to the ship track.

The monomission data are processed as follows. First, gaps in the SSH field are filled by cubic-spline interpolation, then the time-mean SSH is subtracted at each along-track point to form the SSH anomaly. To reduce the effect of noise, the SSH anomaly is smoothed in the along-track direction. A Loess filter (Schlax and Chelton 1992) with a filter wavelength of 47 km is used, allowing direct comparison with the results of Scharffenberg and Stammer (2010, 2011). Finally, the across-track geostrophic velocity is computed as

$$u_\perp(x,0) = \frac{\phi(x+a,0) - \phi(x,0)}{a}, \qquad (1)$$

where a is the sample separation, $\phi(x,y) = g\eta(x,y)/f$ is the normalized surface pressure, g is the gravitational acceleration, f is the Coriolis parameter, η is the SSH anomaly, x is the along-track coordinate, and y is the across-track coordinate. For the TP and $J1$ altimetric missions, $a = 6.3$ km.

The spectrum of the across-track velocity is then estimated as for the ADCP data, now averaging over both passes and all revolutions (Fig. 1). The resulting spectrum has a peak near 300 km and falls off steeply at smaller wavelengths, similar to the ADCP spectrum of across-track velocity. This result is consistent with that of Callies and Ferrari (2013).

c. Tandem mission altimetry

Parallel-track velocity estimates were made possible by the tandem phase of the TP and $J1$ missions. For 3 yr (2002–05), the two satellites were flown quasi simultaneously along parallel ground tracks offset by 157 km at the equator. We use the full 3-yr dataset, comprising 109 revolutions. Again, we use data from the two satellite tracks nearest the *Oleander* ship track (passes 50 and 126) in the latitude range 33°–40°N.

To facilitate direct comparison with the monomission spectrum discussed above, JTP tandem mission data are processed in an analogous way. First, gaps are filled by cubic-spline interpolation, then the time-mean SSH is subtracted at each along-track point to form the SSH anomaly. Next, the SSH anomaly is smoothed in the along-track direction using a Loess filter with a filter wavelength of 47 km. Finally, the along-track velocity is estimated from the SSH anomaly as

$$u_\parallel(x,0) = \frac{\phi(x,a) - \phi(x,0)}{a}, \qquad (2)$$

and the across-track velocity component by (1). For both components, we use a sample spacing equal to the distance between the two satellite tracks at 35°N:

$a = 125$ km. The JTP tandem mission across-track velocity estimate is essentially the same as the monomission estimate, but uses subsampled SSH anomaly. Note that our velocity estimates differ slightly from those of Stammer and Theiss (2004) and Scharffenberg and Stammer (2010, 2011), who estimated velocity using SSH gradients in a direction rotated 45° relative to the satellite track. Here, we use gradients parallel and normal to the satellite track to simplify the analysis in section 3 and to minimize a. Using velocity estimated from the 45° rotated gradients, followed by rotation into along- and across-track coordinates, does not significantly alter our conclusions.

The spectra are estimated as for the monomission data; we again average over both passes and all revolutions. The resulting spectra for along- and across-track velocity are shown in Fig. 1.

d. Comparison

The JTP tandem mission spectra are significantly different from the ADCP and monomission spectra. First, spectral slopes in the high-wavenumber rolloff are closer to k^{-5} than the k^{-3} found from the other sources. Second, the JTP tandem mission spectra have dramatically smaller amplitudes than the spectra from the other sources. The variance in the across-track velocity component is 17×10^{-2} m^2 s^{-2} from monomission altimetry and 14×10^{-2} m^2 s^{-2} from ADCP, compared with only 4.5×10^{-2} m^2 s^{-2} from the JTP tandem mission. Similarly, the variance in the along-track velocity component is 11×10^{-2} m^2 s^{-2} from ADCP, but 2.8×10^{-2} m^2 s^{-2} from the JTP tandem mission.

The ratio of the spectral amplitudes between ADCP and JTP tandem mission depends on the wavelength (Fig. 2). For the across-track component, the JTP tandem mission spectrum approaches the ADCP spectrum at the longest resolved wavelength, but the amplitude is reduced at shorter wavelengths. For the along-track component, however, the JTP tandem mission spectrum is weak by a factor of 2.5 even at 1000-km wavelength. The different high-wavenumber slopes for ADCP and JTP tandem mission spectra are apparent, with the ratio generally following a k^2 power law.

The JTP tandem mission track separation imposes an effective low-pass filter on the observed velocity field, and one typically expects the observed spectrum to approach the true value at wavelengths much longer than the filter scale. The large ratio of ADCP to JTP tandem mission spectral amplitude of along-track velocity, even at wavelengths much longer than the filter scale, illustrates the counterintuitive impact of the finite tandem mission resolution. The following section explains this
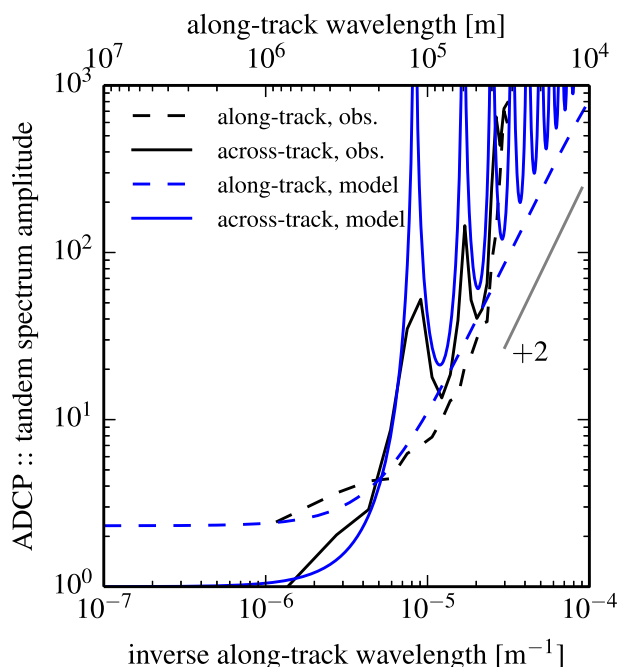
FIG. 2. Ratio of ADCP to JTP tandem mission spectral amplitude (black lines). Across- (solid lines) and along-track (dashed lines) components are shown. Blue lines are for the spectrum model discussed in section 3. A k^2 power law is shown for reference (gray line).

previously unnoticed reduction in spectral amplitude of the along-track velocity.

3. Predicted tandem mission spectra

a. Filtering

The characteristics of the observed tandem mission spectra can be understood by considering the filtering implied by the finite differences taken to compute the geostrophic velocities from SSH. Working in a coordinate system aligned with the satellite track, the geostrophic velocity component normal to an arbitrary unit vector $\mathbf{n}$ is

$$u_{\mathbf{n}}(\mathbf{x}) = \mathbf{n} \cdot \nabla \phi, \qquad (3)$$

where $\mathbf{x} = (x, y)$. In practice, geostrophic velocity is estimated from ϕ at two points separated by a distance a:

$$u_{\mathbf{n}}(\mathbf{x}) = \frac{\phi(\mathbf{x} + a\mathbf{n}) - \phi(\mathbf{x})}{a}. \qquad (4)$$

The two-dimensional Fourier transform is

$$\hat{u}_{\mathbf{n}}(\mathbf{k}) = \int_{-\infty}^{\infty} \int_{-\infty}^{\infty} u_{\mathbf{n}}(\mathbf{x}) e^{i\mathbf{k}\cdot\mathbf{x}} \, dx \, dy \qquad (5)$$

$$= \frac{1}{a} \int_{-\infty}^{\infty} \int_{-\infty}^{\infty} [\phi(\mathbf{x} + a\mathbf{n}) - \phi(\mathbf{x})] e^{i\mathbf{k}\cdot\mathbf{x}} \, dx \, dy$$

$$= \frac{1}{a} (e^{-ia\mathbf{n}\cdot\mathbf{k}} - 1)\hat{\phi}(\mathbf{k}),$$

where $\mathbf{k} = (k, l)$; k and l are the along- and across-track wavenumbers. The spectrum is therefore

$$\langle |\hat{u}_{\mathbf{n}}(\mathbf{k})|^2 \rangle = w(a\mathbf{n} \cdot \mathbf{k}/2)(\mathbf{n} \cdot \mathbf{k})^2 \langle |\hat{\phi}(\mathbf{k})|^2 \rangle, \qquad (6)$$

where angle brackets represent a time average and

$$w(s) = \frac{1 - \cos(2s)}{2s^2} = \frac{\sin^2 s}{s^2} = \text{sinc}^2 s \qquad (7)$$

is a window function introduced by the finite sample spacing.

Because satellite observations only record variations in the along-track direction, the observable spectrum is

$$\langle |\hat{u}_{\mathbf{n}}(k)|^2 \rangle = \int_{-\infty}^{\infty} \langle |\hat{u}_{\mathbf{n}}(\mathbf{k})|^2 \rangle \, dl. \qquad (8)$$

The along-track spectrum of across-track velocity is

$$\langle |\hat{u}_{\perp}(k)|^2 \rangle = w(ak/2)k^2 \int_{-\infty}^{\infty} \langle |\hat{\phi}(\mathbf{k})|^2 \rangle \, dl, \qquad (9)$$

while the along-track spectrum of along-track velocity is

$$\langle |\hat{u}_{\parallel}(k)|^2 \rangle = \int_{-\infty}^{\infty} w(al/2)l^2 \langle |\hat{\phi}(\mathbf{k})|^2 \rangle \, dl. \qquad (10)$$

Comparing (9) and (10) clearly shows the distinct behavior of the spectra of across- and along-track velocity. The spectrum of across-track velocity is simply the low-pass-filtered full spectrum and approaches the full spectrum for $k \ll a^{-1}$. For the spectrum of along-track velocity, on the other hand, the window function affects the estimated spectrum at all wavelengths. The magnitude of the impact of filtering depends on the shape of the SSH spectrum. If the two-dimensional velocity spectrum has significant energy at $l > a^{-1}$, the spectrum of along-track velocity will be reduced, even for $k \ll a^{-1}$. In both cases, the full geostrophic velocity spectrum is recovered as $a \to 0$.

b. Spectrum model

To demonstrate the difference between the spectra of along- and across-track velocity, we must specify an SSH spectrum. While the two-dimensional wavenumber spectrum of SSH has not received much attention, estimates based on ungridded TP altimetry (Glazman et al.
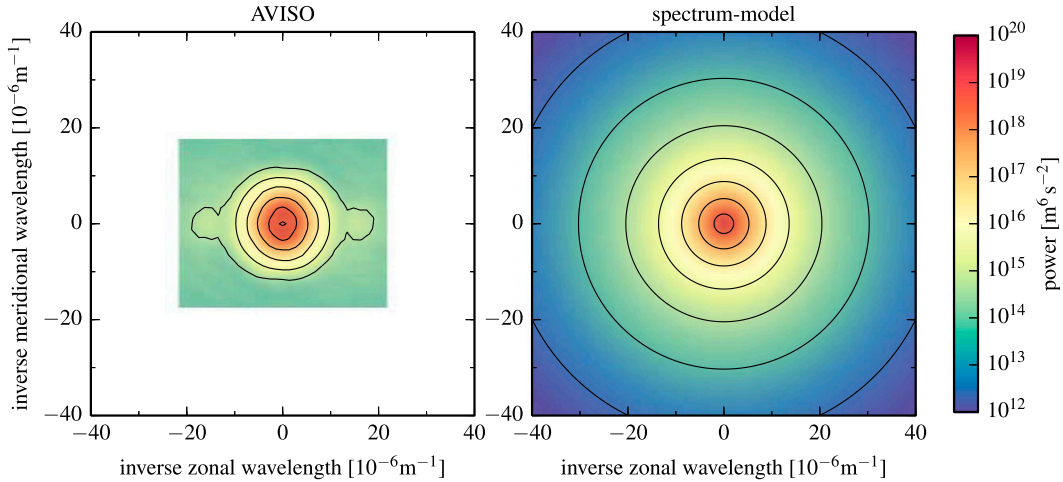
FIG. 3. Two-dimensional wavenumber spectra of the normalized SSH ϕ from the (left) AVISO gridded product and the (right) analytical spectrum model in the Gulf Stream region.

1996) and gridded multimission altimetry (Wortham and Wunsch 2014) exist. Figure 3 shows the two-dimensional wavenumber spectrum of ϕ estimated from the Archiving, Validation, and Interpretation of Satellite Oceanographic data (AVISO) ¼° gridded altimetric product (Ducet et al. 2000) in the Gulf Stream region (33°–40°N, 288°–295°E). The spectrum is computed from weekly SSH anomaly maps after removing the spatial mean, tapering with an isotropic Hamming window, applying the discrete Fourier transform, and averaging over all maps. The AVISO spectrum is an approximately isotropic power law at short scales and flattens at scales much larger than the deformation radius. The domain of the AVISO spectrum is limited by the Nyquist wavenumber of the gridded product. The AVISO spectrum was not presented in section 2 because the mapping procedure will affect the shape of the spectrum, but it still serves as a useful guide in constructing an analytical spectral form.

Based on this limited evidence, consider the simple isotropic wavenumber spectrum

$$\langle|\hat{\phi}(\mathbf{k})|^2\rangle = I(k^2 + l^2 + k_0^2)^{-3}, \tag{11}$$

where $I = 1.6 \times 10^{-9}\,\mathrm{s}^{-2}$ sets the amplitude of the spectrum, and $k_0 = 2\pi/250$ km sets the dominant wavelength. This isotropic spectrum is flat at wavenumbers $k^2 + l^2 \ll k_0^2$ and has a power-law rolloff at wavenumbers $k^2 + l^2 \gg k_0^2$. One-dimensional spectra deduced from this have a k^{-5} rolloff in the SSH spectrum and a k^{-3} rolloff in the velocity spectra. The spectrum of across-track velocity peaks near k_0. The parameters I and k_0 and the rolloff slope are chosen to match the *Oleander* ADCP velocity spectra and would change in different locations.

Equation (11) is a simplified version of the spectrum proposed by Wortham and Wunsch (2014). The spectrum model[1] is shown in Fig. 3.

Figure 4 shows the two-dimensional wavenumber spectra of along- and across-track velocity from the spectrum model. The shading of regions where $\mathbf{n} \cdot \mathbf{k} > a^{-1}$ in Fig. 4 illustrates the impact of the window function in (9) and (10); unshaded areas are passed by the window function, while shaded areas are attenuated.

Integrating each two-dimensional spectrum over all across-track wavenumbers l results in the along-track wavenumber spectrum of the corresponding velocity component. Figure 5 illustrates the impact of the window function on these along-track spectra of along- and across-track velocity. For the across-track velocity, the filtered spectrum ($a = 125$ km) approaches the full spectrum ($a = 0$) for $k \ll a^{-1}$. However, for the along-track velocity, the filtered spectrum is attenuated at all wavelengths. The cusps in the filtered spectrum of across-track velocity are a result of the sinc window function.

Figure 5 shows that the filtered spectrum of along-track velocity from the spectrum model is reduced by a factor of 2.5 at 5000 km, similar to the ratio seen for the JTP tandem mission. The ratio is plotted in Fig. 2. Interestingly, the observed spectral-amplitude ratio of across-track velocity has cusps corresponding to the first two zeros of the sinc function, as predicted. The third cusp and those at the higher wavenumber are smoothed by the along-track Loess filtering applied in the JTP tandem mission analysis.

---

[1] The terminology "spectrum model" is used to distinguish the results from a "spectral model" (GCM formulated in spectral space) or "model spectrum" (spectrum of GCM output).
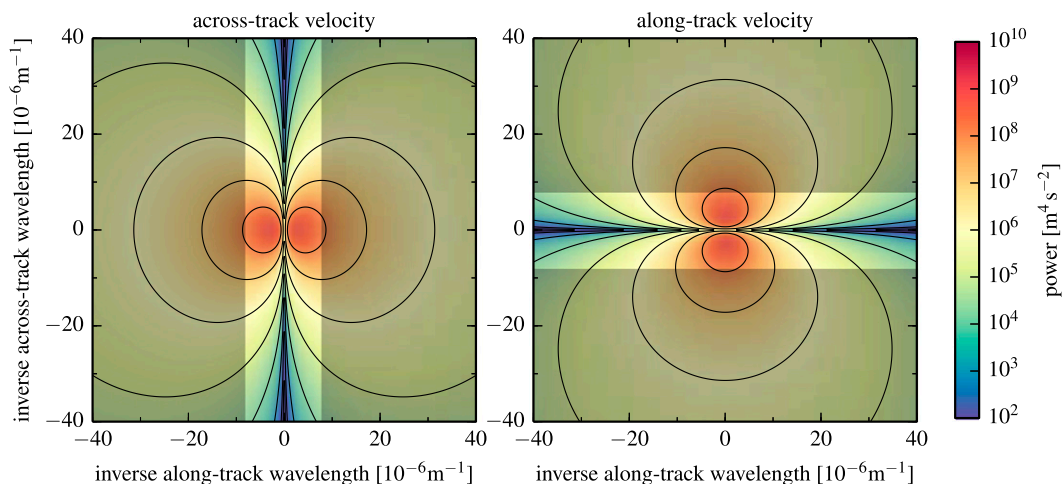
FIG. 4. Two-dimensional wavenumber spectra of (left) across- and (right) along-track velocity from the spectrum model. Shaded areas illustrate the impact of the window function in (9) and (10); see text for details.

c. Spectral slopes

For spectra with an isotropic rolloff, the filter described above steepens spectral slopes at wavelengths much smaller than the sample spacing a by a factor k^{-2}, with cusps added to the spectrum of the across-track velocity (Fig. 5). The filtered spectrum of across-track velocity is the full spectrum multiplied by the filter, which explains the steepening, because $\text{sinc}^2(ak/2)$ has an envelope proportional to k^{-2}. In the appendix, we show that the filter also steepens the spectrum of the along-track velocity, essentially because the envelope of the filter is proportional to l^{-2}.

The range in which this steepening occurs is observed by tandem mission altimetry because the along-track sample spacing is much smaller than the track spacing. Spectral slopes inferred from tandem mission altimetry should be interpreted with this steepening in mind.

d. Test for isotropy

Estimates of the spectra of along- and across-track velocities can be used to test whether the flow is horizontally nondivergent and isotropic (Callies and Ferrari 2013). One needs to take into account that along- and across-track velocities project differently onto the direction of the track. On top of this, when using tandem mission altimetry, one needs to consider the difference in the effect the filter has on the spectra of the two components.

One way to test for isotropy is to construct a two-dimensional isotropic spectrum model from the spectrum of the across-track velocity, which is not affected by the filter at wavelengths longer than the Nyquist

wavelength if differences are taken over the actual sample spacing. If such a constructed spectrum model captures the observed spectrum of across-track velocity, the filtered spectrum of along-track velocity can be inferred and compared to the spectrum estimated from tandem mission altimetry. Inconsistencies point to anisotropies or horizontal divergence. These inferences can be done
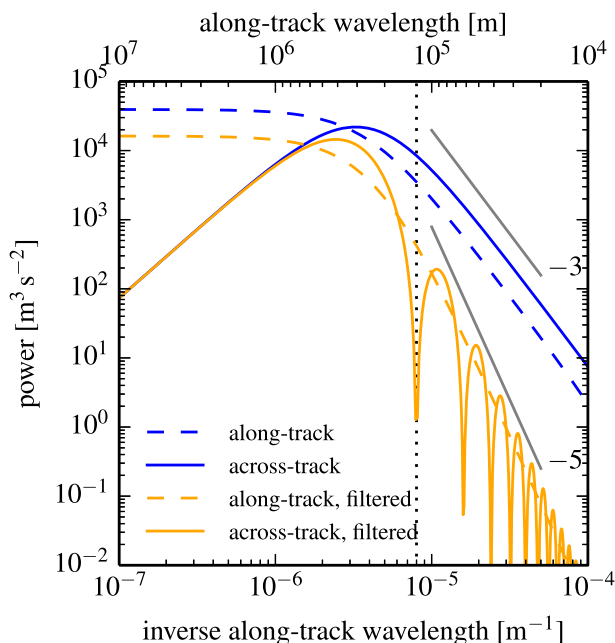

FIG. 5. Analytical spectrum model of one-dimensional across- (solid lines) and along-track (dashed lines) velocity. Full ($a = 0$; blue) and filtered ($a = 125$ km; orange) spectra are shown. The dotted line shows the approximate JTP tandem mission sample spacing of 125 km.

fairly locally in wavenumber space because (i) the one-dimensional spectra at wavenumber k only depends on the two-dimensional isotropic spectrum at wavenumbers $k_h \geq k$ and (ii) if the spectrum is sufficiently steep, the conversion between the one-dimensional spectra and the two-dimensional isotropic spectrum is local. Anisotropies can further be assessed by comparing spectra from ascending and descending tracks. In the next section, we illustrate this test for isotropy in three North Atlantic regions.

4. Regional comparison

Since SSH spectral slope is geographically variable (e.g., Xu and Fu 2012), we use a modified spectrum model with a variable power law:

$$\langle|\hat{\phi}(\mathbf{k})|^2\rangle = I(k^2 + l^2 + k_0^2)^{-n}. \qquad (12)$$

In each region discussed below, a least squares fit of the spectrum model for across-track velocity to monomission observations is performed, resulting in parameters I, k_0, and n. Wavenumber spectra in three representative regions are considered (Fig. 6).

In the Gulf Stream region (33°–40°N, 288°–295°E; passes 50 and 126) the least squares fit yields[2] $k_0 = 2\pi/263$ km, $n = 2.9$. With these parameters, the unfiltered spectrum model is consistent with the monomission spectrum over the full wavenumber range based on the estimated uncertainty. However, the filtered spectrum model is systematically larger than the JTP tandem mission along-track spectrum for wavelengths longer than about 200 km, though marginally within the error bars. At wavelengths shorter than 100 km, the two spectra are nearly indistinguishable. We interpret the inconsistency between predicted and observed along-track spectra as a failure of the spectrum model (12) in this region. Specifically, the flow does not appear to be isotropic at wavelengths longer than about 200 km. This is not surprising: these are the scales of the Gulf Stream, of course a highly anisotropic flow.

The anisotropy can be confirmed by comparing ascending (passes 65 and 141) and descending (passes 50 and 126) tracks. Along-track velocity spectra from ascending and descending diverge at scales longer than 200 km, again indicating anisotropy.

In the central subtropical North Atlantic (33°–40°N, 314°–324°E; passes 48 and 124), the least squares fit yields $k_0 = 2\pi/469$ km, $n = 2.5$. With these parameters, the filtered spectrum model is consistent with the observed spectrum of across-track velocity for wavelengths longer than about 100 km. At shorter wavelengths, the observed spectrum flattens, while the spectrum model by construction maintains a constant spectral slope. The flattening of the observed spectrum is likely due to measurement noise (Stammer 1997). At scales larger than 100 km, where the fit to the spectrum of across-track velocity is good, the filtered spectrum model for along-track velocity matches the JTP tandem mission spectrum very well. The observed spectra are thus consistent with an isotropic flow at wavelengths larger than 100 km. Ascending (passes 63 and 139) and descending (passes 48 and 124) tracks produce nearly indistinguishable spectra.

In the tropical North Atlantic (5°–15°N, 316–323°E; passes 74 and 252), the least squares fit yields $k_0 = 2\pi/986$ km, $n = 2.3$. With these parameters, the unfiltered spectrum model is consistent with the monomission spectrum over the full wavenumber range. However, the filtered spectrum model for along-track velocity is significantly steeper than the JTP tandem mission spectrum. This inconsistency again points to anisotropy. Anisotropy is confirmed by examining ascending (passes 11 and 189) and descending (passes 74 and 252) tracks, which diverge for wavelengths longer than 300 km.

5. Discussion

Wavenumber spectra of near-surface in situ velocity (ADCP) and of geostrophic surface velocity from monomission altimetry have similar shapes and magnitudes in two areas with sufficient in situ data to make a comparison: 33°–40°N, 288°–295°E (Fig. 1) and 25°–35°N, 215°–225°E (cf. Callies and Ferrari 2013). However, in both areas, JTP tandem mission velocity fields capture only ¼ of the velocity variance estimated from other sources, a reduction due to the track spacing of about 125 km. Wavenumber spectra of along- and across-track velocity from the JTP tandem mission behave differently. While the spectrum of across-track velocity is consistent with a simple low-pass filter with 125-km cutoff, the spectrum of along-track velocity is attenuated at all wavelengths. Because of these resolution characteristics, it is incorrect to assume that long wavelength eddies are well resolved by the JTP tandem mission and that only small wavelengths are suppressed by filtering.

The spectral behavior can be understood in terms of the filter window implied by finite sampling of the underlying

---

[2] It should be noted that the slope is weakly constrained because the spectral rolloff is only marginally resolved by current altimeters and the obtained slope is sensitive to how noise is treated (e.g., Xu and Fu 2012).
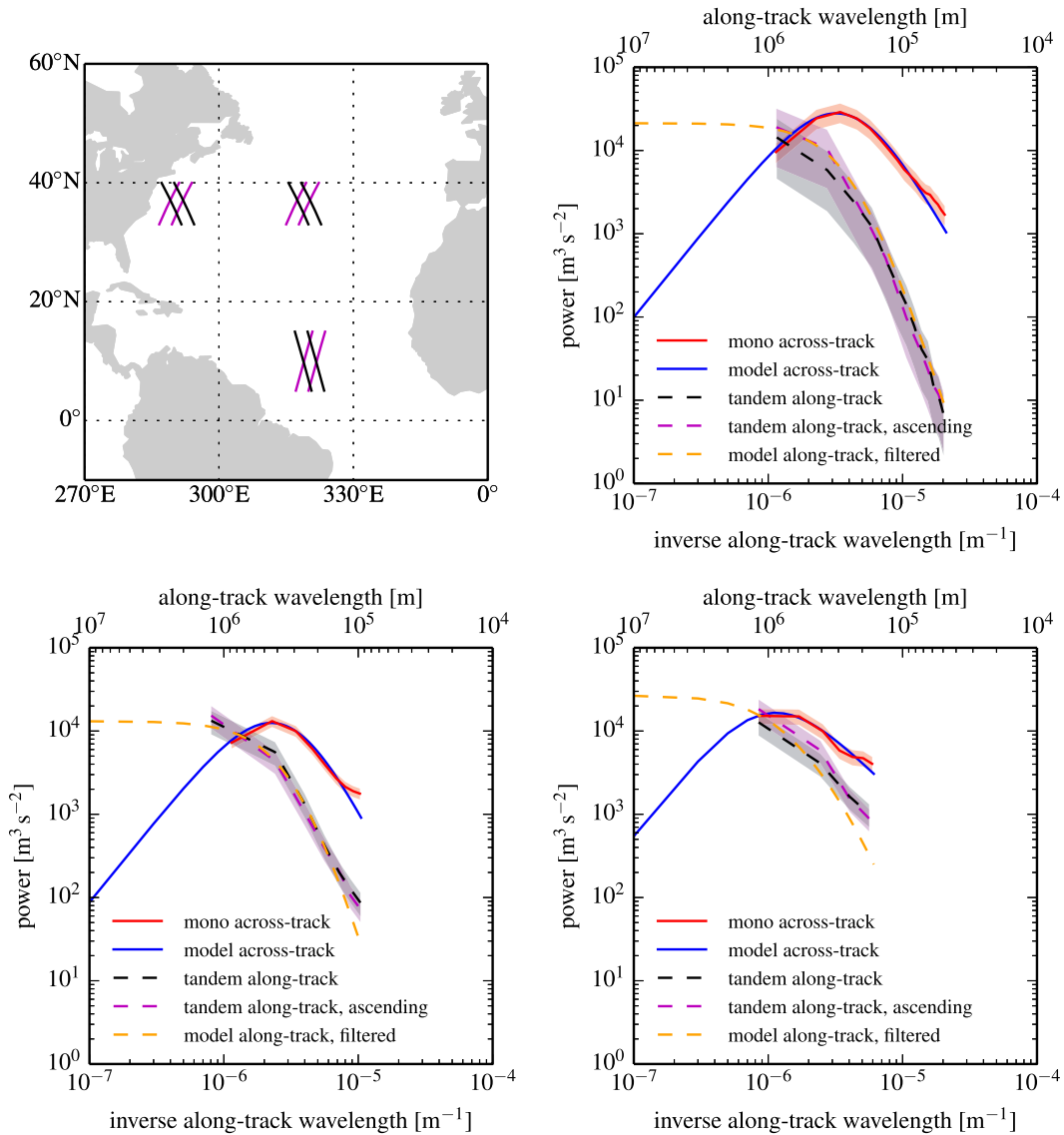
FIG. 6. Comparison of observed spectra with the spectrum model in the (top right) Gulf Stream region (33°–40°N, 288°–295°E), (bottom left) central subtropical North Atlantic (33°–40°N, 314°–324°E), and (bottom right) tropical North Atlantic (5°–15°N, 316°–323°E). In each region, the spectrum model (blue) is fit to the monomission across-track velocity spectrum for descending tracks (red). Then the filtered along-track spectrum model (orange dashed) is compared to observed along-track spectra for descending (black dashed) and ascending (purple dashed) tracks. Shadings indicate the 95% confidence interval. (top left) The map shows the tracks considered.

SSH spectrum. The main result is summarized by (9) and (10): for the across-track velocity, the filter acts parallel to the wavenumber of interest (k axis), while for along-track velocity the filter acts perpendicular to the k axis. Limited resolution of along-track SSH gradients (across-track velocity) only impacts short along-track wavelengths, while limited resolution of across-track SSH gradients (along-track velocity) impacts all along-track wavelengths, so that the spectrum of along-track velocity is reduced at all wavelengths.

Our discussion is in terms of along- and across-track velocity components estimated from along- and across-track SSH gradients, while Scharffenberg and Stammer (2010, 2011) computed velocity in coordinates rotated 45° relative to the satellite track. (These velocities were subsequently rotated to zonal/meridional coordinates in their analysis.) The filtered velocity spectrum in this rotated coordinate system is computed by rotating both the window function and the gradient direction:
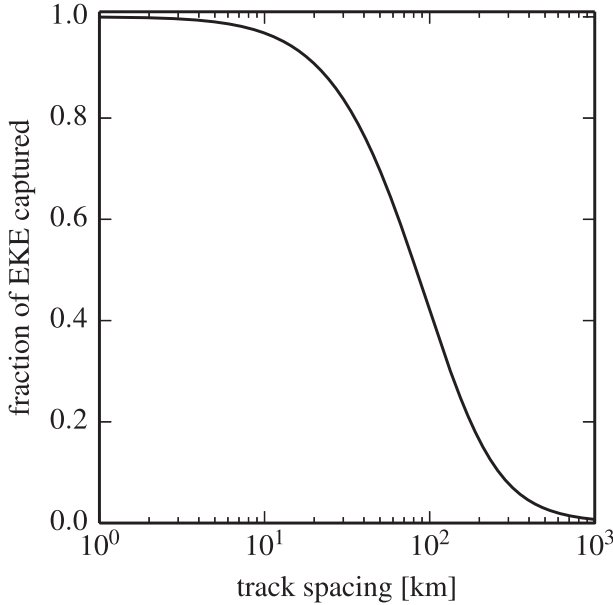
FIG. 7. The fraction of EKE captured by tandem mission sampling as a function of a. This curve is specific to the region 33°–40°N, 288°–295°E and depends on the dominant wavelength through k_0 in (11).

$$\langle|\hat{u}_R(k)|^2\rangle = \int_{-\infty}^{\infty} w\left(a\frac{k+l}{2\sqrt{2}}\right)\left(\frac{k+l}{\sqrt{2}}\right)^2 \langle|\hat{\phi}(\mathbf{k})|^2\rangle\, dl. \quad (13)$$

In this coordinate system, attenuation of the spectrum still extends to all wavelengths.

The eddy kinetic energy (EKE) predicted by the analytical spectrum model,

$$\text{EKE} = \frac{1}{2}\int_{-\infty}^{\infty}[\langle|\hat{u}_\perp(k)|^2\rangle + \langle|\hat{u}_\parallel(k)|^2\rangle]\, dk, \quad (14)$$

depends on the track spacing a (Fig. 7). For an isotropic SSH spectrum, the variance in filtered along- and across-track velocity components will be equal and only depends on the sample spacing a. However, velocity variance is distributed differently in spectral space for the two components (Fig. 5).

Figure 7 shows that the fraction of EKE captured falls off sharply with increasing track spacing from 90% at 20 km to just 30% at 125 km. Note, however, that the fraction of EKE captured by the JTP tandem mission varies geographically (Leeuwenburgh and Stammer 2002, their Fig. 1). With decreased track spacing, a tandem mission would capture more of the EKE. Of course, this must be balanced against the noise limitations; if gradients are taken over too short a distance, the resulting velocity will be dominated by noise. Stammer and Dieterich (1999) concluded that optimal track spacing was

about 0.5°. With a 0.5° track spacing, a tandem mission would capture about 70% of the actual EKE in the Gulf Stream region. Even with this track spacing, spectra of along- and across-track velocity would be impacted by the filter differently, as discussed above. Furthermore, spectral slopes at wavelengths smaller than the track spacing will be steepened by the filtering.

6. Conclusions

The most important outcome of this paper is an understanding of the relationship between kinetic energy sampled by tandem mission altimetry and the satellite track spacing. Spectra of along- and across-track velocity from widely separated satellite tracks behave very differently from each other. While the spectrum of across-track velocity is a low-pass-filtered version of the full spectrum, the spectrum of along-track velocity estimated from a tandem mission is attenuated at all wavelengths. Also, at wavelengths smaller than the track separation, the observed spectral slopes of both velocity components are steeper than the full spectrum by a factor of k^{-2}. Knowledge of the shape of the filter implied by the sampling allows for isotropy tests and may even allow for a reconstruction of the full spectrum.

The best method for reducing the impact of the filtering remains to increase the spatial resolution of the observations, in particular in the across-track direction. The proposed Surface Water and Ocean Topography (SWOT) swath altimeter (Alsford et al. 2007) will address this issue and allow accurate estimation of both velocity components and their wavenumber spectra.

APPENDIX

Steepening of the Tandem Mission Spectrum of Along-Track Velocity

We here show that the spectrum of along-track velocity derived from a finite across-track SSH difference is steepened by a factor k^{-2} at wavelengths shorter than the track spacing. Assume that the underlying SSH spectrum is isotropic and has a power-law rolloff at high

wavenumbers. In (10), we can use the relation between the two-dimensional spectrum and the two-dimensional isotropic spectrum

$$\langle |\hat{\phi}(k_h)|^2 \rangle = 2\pi k_h \langle |\hat{\phi}(\mathbf{k})|^2 \rangle, \qquad \text{(A1)}$$

where $k_h^2 = k^2 + l^2$ is the magnitude of the wavenumber vector, and make a change of variables to arrive at

$$\langle |u_\parallel(k)|^2 \rangle = \frac{1}{\pi} \int_k^\infty w(al/2) l \langle |\hat{\phi}(k_h)|^2 \rangle \, dk_h, \qquad \text{(A2)}$$

where l should be understood as a function of k_h and k. Note that the along-track spectrum at wavenumber k only depends on the two-dimensional isotropic spectrum at larger wavenumbers $k_h \geq k$. For large arguments $s = al/2 \gg 1$, the filter $\text{sinc}^2 s$ oscillates rapidly, so it can be replaced by $1/2s^2$ in the integrand:

$$\langle |u_\parallel(k)|^2 \rangle \approx \frac{2}{\pi a^2} \int_k^\infty \frac{\langle |\hat{\phi}(k_h)|^2 \rangle}{(k_h^2 - k^2)^{1/2}} dk_h. \qquad \text{(A3)}$$

If the two-dimensional isotropic spectrum now follows a power law for $k_h \geq k$, $\langle |\hat{\phi}(k_h)|^2 \rangle = I k_h^{-n}, n > 1$, implying that the unfiltered velocity spectrum falls off like k^{2-n}, the integral can be evaluated to

$$\langle |u_\parallel(k)|^2 \rangle \approx \frac{I}{\pi^{1/2} a^2} \frac{\Gamma(n/2)}{\Gamma[(n+1)/2]} k^{-n}, \qquad \text{(A4)}$$

where Γ is the gamma function. This shows that the filtered spectrum is steeper than the full spectrum by a factor k^{-2}.

REFERENCES

Alsford, D., L.-L. Fu, N. Mognard, A. Cazenave, E. Rodriguez, D. Chelton, and D. Lettenmaier, 2007: Measuring global oceans and terrestrial freshwater from space. *Eos, Trans. Amer. Geophys. Union,* **88,** 253–257, doi:10.1029/2007EO240002.

Batchelor, G. K., 1953: *The Theory of Homogeneous Turbulence.* Cambridge Monographs on Mechanics and Applied Mathematics Series, Cambridge University Press, 197 pp.

Callies, J., and R. Ferrari, 2013: Interpreting energy and tracer spectra of upper-ocean turbulence in the submesoscale range (1–200 km). *J. Phys. Oceanogr.,* **43,** 2456–2474, doi:10.1175/JPO-D-13-063.1.

Ducet, N., P.-Y. Le Traon, and G. Reverdin, 2000: Global high-resolution mapping of ocean circulation from TOPEX/POSEIDON and *ERS-1* and *-2. J. Geophys. Res.,* **105** (C8), 19 477–19 498, doi:10.1029/2000JC900063.

Flagg, C. N., G. Schwartze, E. Gottlieb, and T. Rossby, 1998: Operating an acoustic Doppler current profiler aboard a container vessel. *J. Atmos. Oceanic Technol.,* **15,** 257–271, doi:10.1175/1520-0426(1998)015<0257:OAADCP>2.0.CO;2.

Glazman, R. E., A. Fabrikant, and A. Greysukh, 1996: Statistics of spatial–temporal variations of sea surface height based on Topex altimeter measurements. *Int. J. Remote Sens.,* **17,** 2647–2666, doi:10.1080/01431169608949097.

Leeuwenburgh, O., and D. Stammer, 2002: Uncertainties in altimetry-based velocity estimates. *J. Geophys. Res.,* **107,** 3175, doi:10.1029/2001JC000937.

Leith, C. E., 1971: Atmospheric predictability and two-dimensional turbulence. *J. Atmos. Sci.,* **28,** 145–161, doi:10.1175/1520-0469(1971)028<0145:APATDT>2.0.CO;2.

Scharffenberg, M., and D. Stammer, 2010: Seasonal variations of the large-scale geostrophic flow field and eddy kinetic energy inferred from the TOPEX/Poseidon and *Jason-1* tandem mission data. *J. Geophys. Res.,* **115,** C02008, doi:10.1029/2008JC005242.

——, and ——, 2011: Statistical parameters of the geostrophic ocean flow field estimated from the *Jason-1*–TOPEX/Poseidon tandem mission. *J. Geophys. Res.,* **116,** C12011, doi:10.1029/2011JC007376.

Schlax, M. G., and D. B. Chelton, 1992: Frequency domain diagnostics for linear smoothers. *J. Amer. Stat. Assoc.,* **87,** 1070–1081, doi:10.1080/01621459.1992.10476262.

——, and ——, 2003: The accuracies of crossover and parallel-track estimates of geostrophic velocity from TOPEX/Poseidon and Jason altimeter data. *J. Atmos. Oceanic Technol.,* **20,** 1196–1211, doi:10.1175/1520-0426(2003)020<1196:TAOCAP>2.0.CO;2.

Stammer, D., 1997: Global characteristics of ocean variability estimated from regional TOPEX/POSEIDON altimeter measurements. *J. Phys. Oceanogr.,* **27,** 1743–1769, doi:10.1175/1520-0485(1997)027<1743:GCOOVE>2.0.CO;2.

——, and C. Dieterich, 1999: Space-borne measurements of the time-dependent geostrophic ocean flow field. *J. Atmos. Oceanic Technol.,* **16,** 1198–1207, doi:10.1175/1520-0426(1999)016<1198:SBMOTT>2.0.CO;2.

——, and J. Theiss, 2004: Velocity statistics inferred from the TOPEX/Poseidon–*Jason-1* tandem mission data. *Mar. Geod.,* **27,** 551–575, doi:10.1080/01490410490902052.

Wang, D.-P., C. N. Flagg, K. Donohue, and H. T. Rossby, 2010: Wavenumber spectrum in the Gulf Stream from shipboard ADCP observations and comparison with altimetry measurements. *J. Phys. Oceanogr.,* **40,** 840–844, doi:10.1175/2009JPO4330.1.

Wortham, C., and C. Wunsch, 2014: A multidimensional spectral description of ocean variability. *J. Phys. Oceanogr.,* doi:10.1175/JPO-D-13-0113.1, in press.

Xu, Y., and L.-L. Fu, 2012: The effects of altimeter instrument noise on the estimation of the wavenumber spectrum of sea surface height. *J. Phys. Oceanogr.,* **42,** 2229–2233, doi:10.1175/JPO-D-12-0106.1.